

UniGround: Universal 3D Visual Grounding via Training-Free Scene Parsing

Jiayi Zhang^{1,♣}, Yunheng Wang^{1,♣}, Wei Lu², Taowen Wang¹, Weisheng Xu¹,
Shuning Zhang¹, Yixiao Feng¹, Yuetong Fang^{1,△}, and Renjing Xu^{1,△}

¹ The Hong Kong University of Science and Technology(Guangzhou)

² Shanghai Normal University

Abstract. Understanding and localizing objects in complex 3D environments from natural language descriptions, known as 3D Visual Grounding (3DVG), is a foundational challenge in embodied AI, with broad implications for robotics, augmented reality, and human-machine interaction. Large-scale pre-trained foundation models have driven significant progress on this front, enabling open-vocabulary 3DVG that allows systems to locate arbitrary objects in a given scene. However, their reliance on pre-trained models constrains 3D perception and reasoning within the inherited knowledge boundaries, resulting in limited generalization to unseen spatial relationships and poor robustness to out-of-distribution scenes. In this paper, we replace this constrained perception with training-free visual and geometric reasoning, thereby unlocking open-world 3DVG that enables the localization of any object in any scene beyond the training data. Specifically, the proposed *UniGround* operates in two stages: a Global Candidate Filtering stage that constructs scene candidates through training-free 3D topology and multi-view semantic encoding, and a Local Precision Grounding stage that leverages multi-scale visual prompting and structured reasoning to precisely identify the target object. Experiments on ScanRefer and EmbodiedScan show that *UniGround* achieves 46.1%/34.1% Acc@0.25/0.5 on ScanRefer and 28.7% Acc@0.25 on EmbodiedScan, establishing a new state-of-the-art among zero-shot methods on EmbodiedScan without any 3D supervision. We further evaluate *UniGround* in real-world environments under uncontrolled reconstruction conditions and substantial domain shift, showing training-free reasoning generalizes robustly beyond curated benchmarks.

Keywords: 3D Visual Grounding · Scene Understanding

1 Introduction

3D Visual Grounding (3DVG) is a cornerstone of embodied intelligence that bridges human communication and machine spatial understanding. Specifically, a 3DVG system takes a natural language description as input and precisely

♣ Equal contribution. △ Corresponding authors.

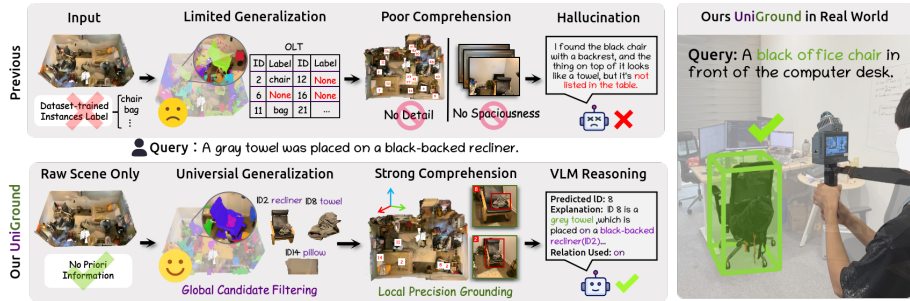


Fig. 1: Conceptual comparison and overview of *UniGround*. **Top:** Existing zero-shot 3D visual grounding pipelines typically construct candidate objects using dataset-trained 3D detectors with prior information, which may degrade under domain shift and affect downstream reasoning quality. **Bottom:** *UniGround* adopts a training-free pipeline consisting of *Global Candidate Filtering* for 2D–3D instance construction and open-vocabulary encoding, followed by the *Local Precision Grounding* for geometric-aware multi-view reasoning with a structured and parsable output. **Right:** Example of real-world deployment in an unseen office scene.

locates the corresponding target object within a 3D scene, enabling a wide range of real-world applications, including augmented reality [21–23], vision-language navigation [32, 39, 44], and robotic perception [13, 14, 16]. Recently, with the rapid rise of large-scale pretrained foundation models, open-vocabulary 3DVG systems are now capable of zero-shot semantic reasoning and flexible natural language instruction following, yet remain largely constrained to in-distribution 3D environments seen during training.

Existing approaches delegate scene parsing to supervised 3D instance segmentation or detection models, whose object proposals serve as the perceptual input to the foundation model (Fig. 1). As these 3D perception modules are trained on closed-set, domain-specific datasets, they inherently restrict which objects and spatial configurations can be surfaced as candidates, regardless of how semantically capable the downstream model is. In other words, the open-vocabulary capability of such systems is limited to the language reasoning side, while the 3D perception front-end remains fundamentally closed-set. Therefore, 3DVG systems relying on such pretrained 3D modules face two compounding limitations: ❶ **Limited Generalization:** Reliance on supervised 3D segmentation models trained on in-domain data limits the system’s ability to generalize to open-set object categories and unseen environments, rendering any out-of-distribution object undetectable to the grounding pipeline; ❷ **Poor Comprehension:** Single-perspective visual prompting provides impoverished spatial and semantic context to the VLM, leaving fine-grained object attributes and global scene-level relationships insufficiently grounded, ultimately undermining localization accuracy.

We argue that the bottleneck lies, instead, in how well the model sees. 3D scene understanding can be decomposed into geometric perception, which cap-

tures spatial structure and inter-object relationships, and semantic reasoning, which aligns natural language descriptions with visual concepts. While many existing works aim to solve these two problems at once using a larger and more powerful supervised 3D segmentation model, this demands expensive 3D annotations and constraining geometric perception within the semantic biases inherited from pretraining. Counterintuitively, we demonstrate that moving away from domain-specific 3D models is precisely the key to unlocking full-scene generalization in 3DVG. Motivated by this, we propose *UniGround*, a framework that fundamentally departs from the prevailing paradigm by decoupling geometric perception from semantic reasoning into two distinct stages. *UniGround* constructs a topology-aware scene representation by integrating 2D segmentation with spatial topology graphs and multi-view RGB information, requiring no 3D supervision of any kind. A training-free reasoning framework then grounds this representation through multi-dimensional context prompting, enabling the VLM to perform precise spatial reasoning. Empirically, *UniGround* attains 46.1/34.1 Acc@0.25/0.5 on ScanRefer and transfers to EmbodiedScan with 28.7 Acc@0.25, validating training-free open-world grounding across unseen scenes. The contributions are:

- We introduce the Global Candidate Filtering stage, a training-free approach that extracts scene-level prior information from multi-view RGB inputs without any 3D supervision, enabling open-world generalization across unseen scenes.
- We introduce the Local Precision Grounding stage, which employs a multi-scale visual prompting reasoning chain to equip the VLM with fine-grained spatial context for precise object localization in complex scenes.
- We prove that decoupling geometric perception from semantic reasoning, without relying on any domain-specific 3D model, is sufficient to achieve full-scene generalization, high localization accuracy, and real-world deployability in 3DVG – all in a fully zero-shot fashion.

2 Related work

2.1 Supervised 3D Visual Grounding

The inception of supervised 3D Visual Grounding can be traced back to pioneering works such as ScanRefer [3] and ReferIt3D [1], which established the task of localizing specific objects by aligning 3D scenes with natural language descriptions under full supervision. Prior arts mainly adopted a decoupled "detect-match" pipeline [1, 3, 9, 15, 40, 46], where a pre-trained 3D detector first generates object proposals and a cross-modal matching model subsequently ranks candidates against the query. While conceptually aligned with our decoupling philosophy, this paradigm delegates geometric perception to a supervised 3D detector, which requires expensive 3D annotations for training and inherits the well-known generalization limitations of domain-specific 3D models, including sensitivity to point cloud density and scene distribution shift. As a result, this

paradigm is sensitive to scene distribution shift and variations in point cloud density, and generalizes poorly to environments outside its training distribution.

More recent research has shifted toward unified end-to-end architectures that jointly learn 3D geometric and linguistic representations [5–7, 19, 26, 27, 29, 31], enabling deeper multimodal fusion so that language cues can directly guide feature extraction and spatial reasoning for more context-aware localization. Yet regardless of architectural sophistication, these models remain bounded by the 3D scene distributions seen during pretraining: their geometric perception is shaped by the specific point cloud statistics, object categories, and spatial configurations of curated indoor benchmarks, and does not transfer to scenes with different density, scale, or structural characteristics. Current open-vocabulary 3DVGs [8, 10, 17, 18, 20, 35] attempt to sidestep annotation costs by leveraging LLM/VLM priors for grounding, but geometric perception remains dependent on pretrained 3D components that carry the same distributional constraint, i.e., achieving zero-shot in language while remaining few-shot in geometry. UniGround addresses this at its root by replacing domain-specific 3D models with a training-free geometric perception stage, achieving genuine cross-scene generalization and precise semantic–spatial grounding without any 3D supervision.

2.2 Zero-shot 3D Visual Grounding

Zero-shot 3DVG aims to leverage the reasoning and cross-modal alignment capabilities of foundation models to overcome the limited generalization of supervised methods. However, the majority of existing approaches [8, 10, 17, 18, 20, 35] remain zero-shot only in the linguistic sense: they rely on a pretrained 3D instance segmentation model to construct an object lookup table that supplies bounding boxes and semantic labels, reducing grounding to a filtering problem over pre-defined object candidates. This design enables open-vocabulary query handling, but geometric perception remains anchored to in-domain 3D supervision, meaning these methods generalize across language, but not across scenes. For instance, SeeGround [17] and View-on-Graph [20] combine VLMs with globally rendered views for stronger spatial reasoning, while VLM-Grounder [35], SeqVLM [18], and SPAZER [10] further incorporate native RGB observations to preserve local semantic and spatial cues. Yet all of these works inherit the same distributional constraints from their underlying 3D segmentation backbone, limiting their applicability to scenes well-covered by the training distribution. UniGround addresses this gap by replacing the segmentation-based perception stage entirely with a training-free geometric perception pipeline, achieving grounding that is zero-shot in both language and scene without any 3D supervision of any kind.

3 Methodology

We begin by defining the task in Section 3.1, then introduce *UniGround*, a training-free framework for open-world 3DVG that parses any scene without

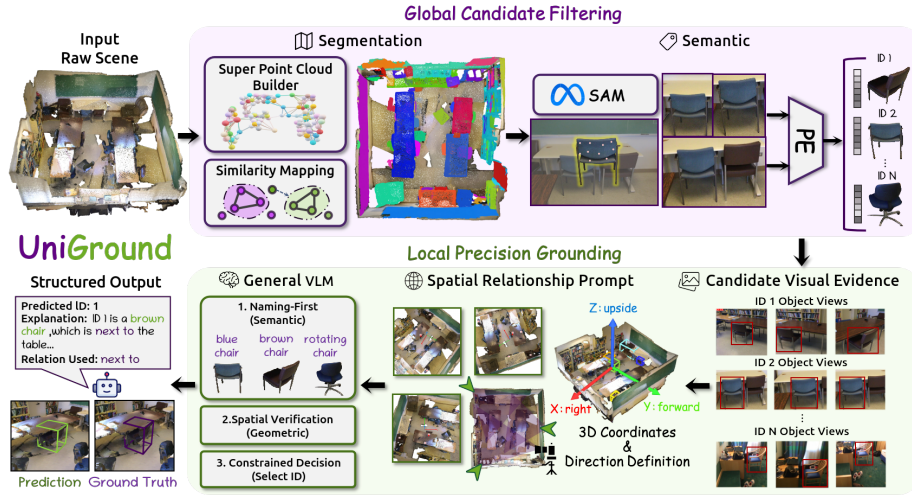


Fig. 2: Overview of *UniGround*. Given raw scene observations and a language query, *UniGround* performs **Stage 1: Global Candidate Filtering** to retrieve a compact candidate set, followed by **Stage 2: Local Precision Grounding**, which localizes the target by jointly reasoning over global scene context for spatial verification and candidate-centric visual evidence for semantic identification.

task-specific supervision. As illustrated in Fig. 2, the system takes raw scene observations as input, including first-person RGB-D sequences with camera poses, colored point clouds, and natural language instructions. The framework operates in two stages: Global Candidate Filtering (Stage One, 3.2), which isolates potential objects corresponding to the instruction, and Local Precision Grounding (Stage Two, 3.3), which performs fine-grained localization on these candidates to identify the target object. The two stages are referred to as Stage One and Stage Two throughout the remainder of this section.

3.1 Problem Formulation

The goal of the zero-shot 3D Visual Grounding (3DVG) task is to localize the target object within the 3D scene based on the textual description, without requiring scene-specific training or fine-tuning. The output is a directed 3D bounding box (bbox) that identifies the object’s location and dimensions. We represent the 3D scene as a colored point cloud, where each point has XYZ coordinates and RGB color attributes. This scene is accompanied by a sequence of first-person view images containing RGB, depth, and pose information. The system takes these visual inputs along with a natural language query to identify and bound the target object.

3.2 Stage One: Global Candidate Filtering

This module is responsible for dividing the scene into distinct units and performing an initial selection of objects based on the instructions provided. Existing Zero-Shot 3D Visual Grounding approaches are contingent upon supervised 3D segmentation models to partition scenes and assign categorical labels. Although effective in controlled settings, these methods are inherently constrained by their reliance on supervised training data, which impedes their capacity to generalize to novel, unseen environments. To address this limitation, we draw inspiration from the Topological Clustering Strategy in HERO [33], which leverages the strengths of 2D models and spatial topology for 3D instance segmentation while assigning semantic categories for each instance through multi-angle RGB images and a design to fill in missing information.

Segmentation. We adopt a 2D-to-3D lifting strategy [28,33,36]: 2D instance masks are projected onto the 3D point cloud and aggregated into complete instances by merging geometrically connected regions with consistent semantics [24,41,42]. As shown in Fig. 2, the input point cloud is first partitioned into superpoints via VCCS [24] and region growing [42], forming compact geometric primitives that preserve local continuity, planar smoothness, and appearance consistency. We then estimate the affinity between each pair of adjacent superpoints by identifying all camera views that jointly observe both regions, applying SAM [12] to generate 2D instance masks, and evaluating joint visibility and semantic consistency. These factors are aggregated into a pairwise similarity $C_{i,j}$, defined as:

$$C_{i,j} = \frac{1}{m} \sum_{k=1}^m \underbrace{\frac{|i^k|_{\text{vis}} |j^k|_{\text{vis}}}{|i| |j|}}_{\text{joint visibility}} \cdot \underbrace{\frac{\mathbf{f}_i^k \cdot \mathbf{f}_j^k}{\|\mathbf{f}_i^k\|_2 \|\mathbf{f}_j^k\|_2}}_{\text{semantic consistency}}, \quad (1)$$

where i and j are adjacent superpoints, m is the number of views jointly observing both, $|i^k|_{\text{vis}}$ and $|i|$ denote the visible and total pixel counts of superpoint i in view k , and $\mathbf{f}_i^k \in \mathbb{R}^n$ is the feature vector of superpoint i over the n SAM-generated instance masks in view k , with \mathbf{f}_j^k defined analogously. The resulting similarities drive a progressive merging scheme [36], where merging sensitivity is dynamically adjusted at each stage to fuse smaller regions first and progressively recover complete object instances.

Semantic. Instance segmentation can yield geometric attributes, but not semantic attributes, requiring semantic labels to enable query-driven object selection. For each candidate object, we apply a defect correction and multi-scale fusion strategy to obtain robust semantic embeddings. A key challenge is that 3D reconstruction artifacts and incomplete superpoint merging often produce objects with ragged boundaries or missing surfaces; encoding semantics directly from such imperfect geometry would incorporate background clutter or occluded regions into the embedding, corrupting the representation. To address this, we identify the corresponding RGB images via depth and pose information, and project the downsampled point cloud onto 2D pixels, which serve as SAM

prompts for conditional re-segmentation. This recovers clean object boundaries in 2D that the 3D geometry alone cannot guarantee. The corrected regions are then cropped and progressively rescaled back to the original image resolution. This multi-scale sequence captures both fine-grained local texture and broader contextual cues, which is particularly important for objects whose identity depends on surrounding context, such as a monitor distinguished from a painting by the desk beneath it. The sequence is encoded by a Perception Encoder (PE) [2], whose joint visual-language embedding space enables direct similarity computation between image and text representations without requiring a separate alignment step. Encodings from multiple viewpoints are averaged to suppress view-dependent noise and produce a stable semantic embedding for each candidate. At query time, the user instruction is embedded with the same PE model, and cosine similarity is computed against all candidate embeddings. The top candidates are then retained through Global Candidate Filtering for downstream processing.

3.3 Stage Two: Local Precision Grounding

This module aims to further refine the localization of the target object by precisely selecting it from the candidate set filtered in Stage One. Existing zero-shot 3DVG methods typically follow two prompting paradigms. At the macro level, some render 3D scenes into 2D projections to capture global spatial context [17, 20], enabling reasoning about relative positions and long-range dependencies. In contrast, others focus on the micro level, using multi-view renderings or RGB images of individual candidates to capture fine-grained semantic details and local relationships that global projections may miss [10, 18]. However, this dichotomy entails a fundamental trade-off: macro-level prompts retain global geometry but dilute fine-grained semantics, whereas micro-level prompts preserve instance semantics but weaken global spatial context, undermining robust and stable localization. To bridge this gap, we combine Spatial Relationship Prompts with Candidate Visual Evidence under a Chain-of-Thought prompting procedure, encouraging the model to cross-reference complementary visual evidence at both levels within a unified decision process, yielding localization predictions that are both interpretable and accurate.

Spatial Relationship Prompt. Point-cloud renderings are highly sensitive to camera pose, and suboptimal viewpoints can yield visually uninformative projections while introducing misleading global spatial cues that derail the VLM’s relation reasoning. To recover global spatial relations that are ambiguous under local crops, we render the scene from a set of constrained camera poses (Fig. 3). The key idea is to anchor all viewpoints to a unified reference center and sample multi-view observations by orbiting

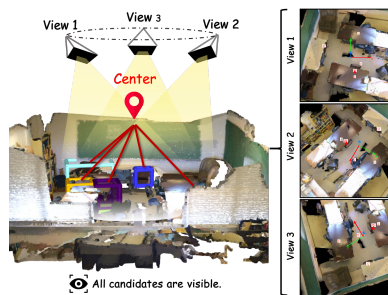


Fig. 3: Orbit rendering and candidate views.

the camera around it with minimum radius and height constraints to ensure stable, non-degenerate views. Formally, the camera position is defined as:

$$\text{cam}(\theta) = \frac{1}{K} \sum_{i=1}^K c_i + [r \cos \theta \ r \sin \theta \ h]^\top, \quad h \geq h_{\min}, \ r \geq r_{\min}, \quad (2)$$

where K is the number of candidate 3D boxes and $c_i \in \mathbb{R}^3$ is the center of the i -th candidate, θ is the azimuth angle, r is the orbit radius (horizontal distance), and h is the camera height. We enforce $r \geq r_{\min}$ and $h \geq h_{\min}$ to avoid degenerate close-up or low-altitude viewpoints. Additionally, to better facilitate spatial understanding, we overlay a global coordinate frame to ground directional cues in the instruction and assign each candidate object a unique visual ID for unambiguous reference.

Candidate Visual Evidence. Directly rendering local object crops from point clouds into 2D images often yields unstable object appearances due to sparsity, occlusion, and viewpoint sensitivity, which can obscure discriminative visual attributes and lead to semantic loss. To mitigate this issue, we directly use the native RGB observations captured from the first-person view as the basis for constructing object-level local semantics. Specifically, for each candidate object, we select l views such that the object occupies a large pixel proportion in each image, while the pairwise spatial distances among the selected viewpoints are maximized, thereby preserving both visual detail and cross-view complementarity. Finally, to explicitly guide the model’s attention to the target object region, we overlay a bounding box on the object in each selected image, providing localized visual emphasis for more reliable semantic classification.

Algorithm 4. General VLM reasoning for local precision grounding.

Input: Query q ; candidate set $\mathcal{C} = \{i\}_{i=1}^K$; global renders \mathcal{G} ;

candidate views $\mathcal{V} = \{\mathcal{V}_i\}_{i=1}^K$

Output: Selected index $\hat{i} \in \{1, \dots, K\}$ with explanation e

1. Define axis-language mapping Φ consistent with the rendered coordinate frame.
2. **Semantic reasoning (naming-first):**
 For each candidate, infer $\text{name}_i \leftarrow \text{VLM}(\mathcal{V}_i)$.
 Match the query target with $m \leftarrow \text{MATCHTARGET}(q, \{\text{name}_i\})$.
3. **Spatial reasoning:**
 Parse $\mathcal{R} \leftarrow \text{PARSERELATIONS}(q)$.
 Infer $(\hat{i}, e) \leftarrow \text{VLM}(\mathcal{G}, \mathcal{R}, \Phi, \mathcal{C})$.
4. **Closed-loop correction:**
 If $\hat{i} \notin \mathcal{C}$ or $\text{INCONSISTENT}(m, \hat{i}, q)$, re-query with
 $(\mathcal{G}, \mathcal{V}_{\hat{i}}, \mathcal{R}, \Phi, \mathcal{C})$.
5. Project back to the valid candidate set with
 $\hat{i} \leftarrow \text{PROJECTTOCANDIDATES}(\hat{i}, \mathcal{C})$, then return \hat{i}, e .

General VLM. Building upon refined visual cues, the challenge lies in effectively guiding the model to utilize these visual signals for reasoning, capitalizing

on the advantages of both macro and micro visual processing, while mitigating its inherent limitations, and establishing a closed-loop reasoning process. To address this challenge, we designed a process: (1) **Semantic Reasoning**: Guiding the model to analyze object semantics using fine-grained semantic classification visual prompts, assisting in aligning the model with the query referent; (2) **Spatial Reasoning**: Guiding the model to analyze spatial relationships between objects using spatial relationship visual prompts, assisting the model in aligning with the directional information in the instruction. (3) **Correction Reasoning**: Guiding the model to scrutinize the initially inferred object and perform closed-loop re-evaluation and reasoning when inconsistencies are detected, mitigating hallucinations and reducing inconsistencies in the reasoning process. The complete reasoning protocol is formalized in Algorithm 4. The detailed prompts are provided in the Appendix 1.

4 Experiments

4.1 Experimental Details

Evaluation Benchmark. For our evaluation, we utilize the ScanRefer dataset, comprising 51,500 descriptions across 800 ScanNet scenes, with a validation set of 9,508 queries, which is widely regarded as a standard benchmark for accuracy assessment. To evaluate generalization across different scene distributions, we use the EmbodiedScan dataset, which contains over 5,000 scans, 1 million language prompts, and 160,000 3D-oriented bounding boxes. For our experiments, we select over 6,000 tasks from 30 ARKitScenes. Additionally, to evaluate performance in real-world settings, we construct a benchmark consisting of four indoor environments: Office, Lounge, Corridor, and Conference. In each environment, we perform 25 query tasks covering a total of five distinct target objects.

Implementation Details. In Stage One, instance segmentation is performed using a progressive-growing aggregation strategy, where the similarity threshold is linearly relaxed from 0.9 to 0.5 over five stages to ensure robust consolidation from small to large regions. Semantic labeling leverages a multi-modal Perception Encoder, with 10 candidate viewpoints sampled per object to generate comprehensive semantic embeddings. Candidate selection is then performed by choosing the top- u objects, with $u = 5$ for ScanRefer and $u = 10$ for EmbodiedScan, balancing coverage and precision. In Stage Two, three global viewpoints are selected for the Spatial Relationship Prompts to provide stable scene-level spatial context, while three local viewpoints per candidate are used for Candidate Visual Evidence to capture fine-grained semantic details and reinforce object-centric reasoning. This configuration enables the model to leverage global spatial verification and local semantic discrimination jointly, ensuring accurate and robust target localization.

4.2 Evaluation in Simulated Environments

As shown in Tab. 1, we categorize existing approaches into three groups: Fully Supervised Learning-Based Methods, Open-Vocabulary Zero-Shot Methods, and

Table 1: Evaluations of 3DVG on the ScanRefer Validation Set and a Subset of the EmbodiedScan Set within ARKitScenes.

Method	Venue	Agent		Prior Info.		ScanRefer		EmbodiedScan
		Rep.	VLM	Bbox	Class	Acc@0.25 ↑	Acc@0.5 ↑	Acc@0.25 ↑
Fully Supervised Learning-Based Methods								
ScanRefer [3]	ECCV'20	✗	✗	-	-	39.0	26.1	12.9
InstanceRefer [38]	ICCV'21	✗	✗	-	-	40.2	32.9	-
3DVG-T [43]	ICCV'21	✗	✗	-	-	45.9	34.5	-
BUTD-DETR [9]	ECCV'22	✗	✗	-	-	52.2	39.8	22.1
L3Det [45]	arXiv'23	✗	✗	-	-	-	-	23.1
EDA [34]	CVPR'23	✗	✗	-	-	54.6	42.3	-
3D-VisTA [46]	ICCV'23	✗	✗	-	-	50.6	45.8	-
G ³ -LQ [31]	CVPR'24	✗	✗	-	-	56.0	44.7	-
Embodied Perceptron [30]	CVPR'24	✗	✗	-	-	-	-	25.7
MCLN [27]	ECCV'24	✗	✗	-	-	57.2	45.7	-
ConcreteNet [29]	ECCV'24	✗	✗	-	-	50.6	46.5	-
TSP3D [5]	CVPR'25	✗	✗	-	-	56.5	46.7	-
Open-Vocabulary Zero-Shot Methods								
ZSVG3D [37]	CVPR'24	✗	GPT-4V	✓	✓	36.4	32.7	-
VLM-Grounder [35]	CoRL'24	✗	GPT-4V	✓	✓	51.6	32.8	-
SeeGround [17]	CVPR'25	✗	Qwen2-VL	✓	✓	44.1	39.4	7.7
VoG [20]	AAAI'26	✗	Qwen2-VL	✓	✓	44.8	40.3	-
SeqVLM [18]	ACM'25	✗	Doubao-1.5	✓	✓	55.6	49.6	0.9
SPAZER [10]	NeurIPS'25	✗	GPT-4o	✓	✓	57.2	48.8	-
Open-World Zero-Shot Methods								
LERF [11]	ICCV'23	CLIP	✗	✓	✓	4.8	0.9	-
OpenScene [25]	CVPR'23	CLIP	✗	✓	✓	13.2	6.5	-
LLM-G [4]	ICRA'24	✗	GPT-3.5	✓	✓	14.3	4.7	-
LLM-G [4]	ICRA'24	✗	GPT-4T	✓	✓	17.1	5.3	-
Ours	Ours	PE	GPT-5	✗	✗	46.1	34.1	28.7

Open-World Zero-Shot Methods, and benchmark our method against state-of-the-art techniques across these categories. Different from prior works that report results separately on Unique and Multiple subsets, we focus on overall performance across the entire dataset to better reflect practical applicability in realistic scenarios, where agents must operate robustly under diverse and unconstrained conditions.

UniGround exhibits robust cross-scene generalization. As detailed in Tab. 1, UniGround achieves the best performance among open-world zero-shot methods on ScanRefer, and its advantage becomes substantially larger under cross-dataset transfer to EmbodiedScan. Specifically, UniGround surpasses the runner-up LLM-G [4] by 29.0% / 28.8% at Acc@0.25/0.5 on ScanRefer, and further exceeds representative open-vocabulary baselines such as SeeGround [17] by 21.0% on EmbodiedScan. Remarkably, our training-free framework even outperforms the fully supervised Embodied Perceptron [30] by 3.0% on EmbodiedScan, highlighting strong generalization to unseen environments.

This generalization is primarily driven by the training-free Global Candidate Filtering (Stage 1), which constructs geometry-consistent candidates without relying on dataset-specific 3D segmentation priors. As illustrated in Fig. 5, prior methods often produce fragmented or noisy instances under domain shift, which then contaminates candidate proposals and causes downstream grounding failures. In contrast, UniGround yields coherent object candidates via geometry-driven superpoint aggregation and multi-view semantic verification, providing a stable candidate set for Stage 2 and enabling reliable grounding in unseen scenes.

UniGround exhibits robust spatial-semantic scene understanding. Beyond its superior cross-dataset transferability, UniGround demonstrates ad-

vanced scene-level reasoning capabilities compared to existing open-vocabulary grounding frameworks. As reported in Tab. 1, UniGround consistently outperforms representative recent baselines, achieving significant absolute gains of +9.7%, +2.0%, and +1.3% in Acc@0.25 over ZSVG3D [37], SeeGround [17], and VoG [20], respectively. Notably, while SPAZER [10] currently maintains a performance lead on the ScanRefer benchmark, it relies heavily on external prior information (e.g., 3D Bbox and Class priors) to constrain the search space. In sharp contrast, UniGround achieves competitive performance without any dataset-specific 3D segmentation or category-level priors.

We attribute this substantial performance leap to our specialized Stage Two scene-understanding prompting design, which effectively reconciles the two distinct failure modes inherent in conventional approaches. Specifically, previous methods often struggle with a trade-off: global-contextual prompts tend to sacrifice fine-grained semantic details to maintain long-range relations, whereas local-object extraction focuses on appearance cues while neglecting crucial scene-level spatial constraints. In contrast, UniGround mitigates these limitations by performing explicit inference-time verification over observable scene structures. By seamlessly integrating global spatial context with object-centric visual evidence, our reasoning-centric design substantially reduces referential ambiguity. This ensures superior robustness even in cluttered environments populated with visually similar distractors.

4.3 Evaluation in Real-world Environments

We evaluate our method in real-world indoor environments against the latest open-source and representative open-vocabulary zero-shot 3DVG approaches, namely SeeGround [17] and SeqVLM [18], to provide a comprehensive assessment across methodological paradigms. The evaluation is conducted in four distinct environments: Conference, Lounge, Office, and Corridor. In each environment, we perform 25 query tasks covering a total of five distinct target objects. The detailed experimental setups are provided in the Appendix 2.

UniGround demonstrates robust real-world deployability. As reported in Tab. 2, UniGround consistently outperforms SeeGround [17] and SeqVLM [18] across all four real-world environments, achieving 40% and 36% higher average success rates, respectively. In challenging spaces such as Corridor and Conference where baseline performance nearly collapses, UniGround still maintains a robust average success rate of 30.0%.

This robustness is rooted in UniGround’s training-free design across *both* stages. In real scenes, sensor noise, partial observations, and pose drift frequently break the dataset-specific assumptions of segmentation-based pipelines, resulting in unstable or incomplete instances and thus brittle candidate proposals.

Table 2: 3DVG results in real-world environments

Method	Conference	Lounge	Office	Corridor
SeeGround [17]	2/25	0/25	5/25	0/25
SeqVLM [18]	0/25	0/25	3/25	0/25
Ours	10/25	13/25	15/25	5/25

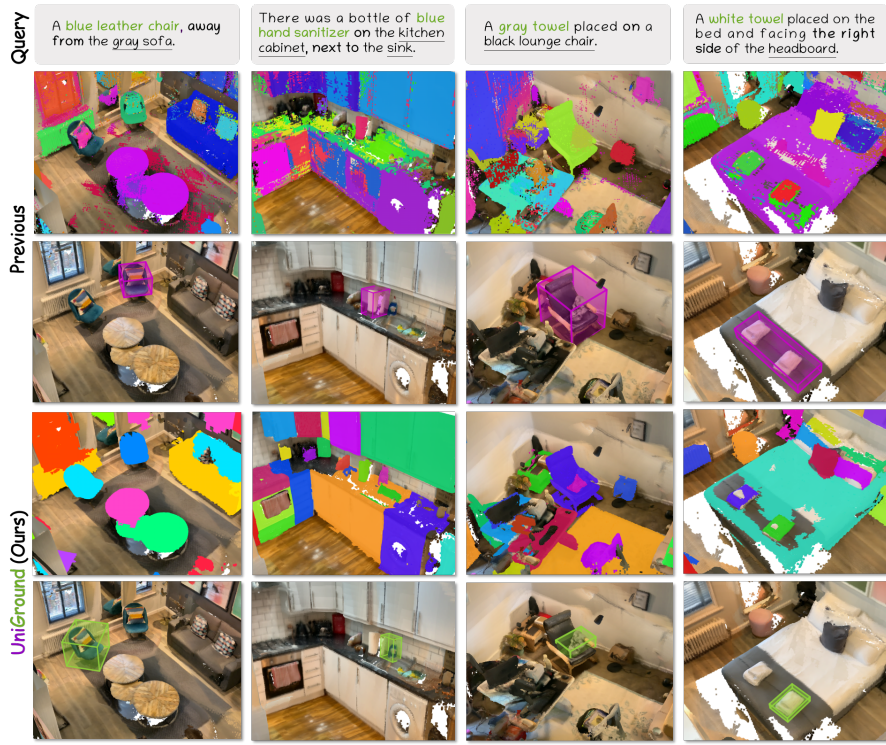


Fig. 5: Qualitative comparison on the cross-dataset ARKitScene benchmark. Purple boxes denote failures and green boxes denote correct grounding.

Stage 1 addresses this by constructing geometry-consistent candidates via superpoint aggregation and multi-view semantic verification, which stabilizes the candidate set under uncontrolled reconstructions. Building upon reliable candidates, Stage 2 performs inference-time verification by jointly reasoning over global spatial context and object-centric visual evidence, effectively preventing error accumulation from noisy perception to final grounding. Fig. 6 shows representative examples where UniGround localizes targets reliably despite clutter and reconstruction artifacts.

4.4 Ablation Study

To evaluate the contribution of each component within UniGround, we conduct ablation studies on 1,059 tasks randomly sampled from the ScanRefer dataset, covering 20 distinct ScanNet scenes.

Effect of the Number of Candidate Objects in Global Candidate Filtering. As the initial stage of our hierarchical framework, Global Candidate Filtering is deterministic for the overall performance, as the search space for the subsequent fine-grained localization (Stage 2) is strictly confined to the filtered

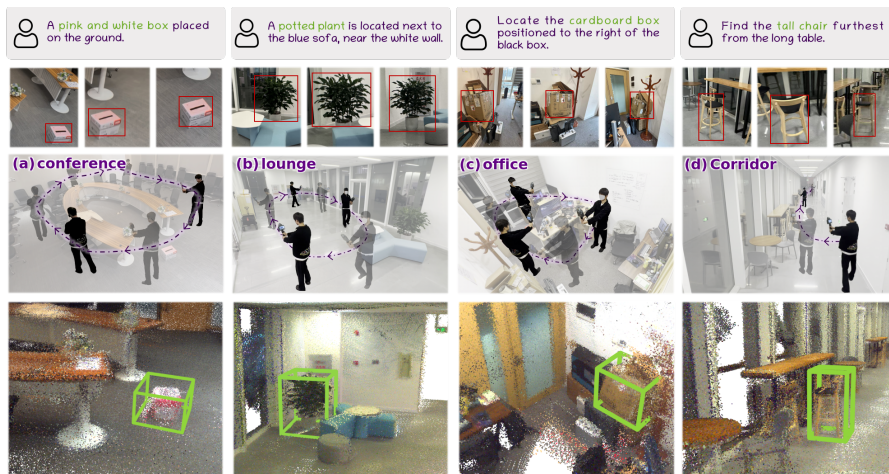


Fig. 6: Real-world qualitative results in unseen indoor scenes under capture noise and layout shift.

candidates. While a larger candidate set enhances global recall and minimizes the risk of target omission, it imposes a significant computational burden on Stage 2, particularly in terms of token consumption and inference latency.

As illustrated in Fig. 7, localization performance exhibits a three-stage evolution as N scales. In the *Rapid Growth* phase ($N \leq 5$), $\text{Acc}@0.25$ surges from 28.5% to 64.7%, indicating that a sufficient candidate pool is vital for global context coverage. However, this gain diminishes in the *Slow Growth* phase ($N \in [5, 10]$) and eventually reaches a *Saturation Phase* beyond $N = 10$, where further increments yield marginal improvements (e.g., $\sim 6\%$ from $N = 10$ to 20). We select $N = 5$ as the optimal trade-off between accuracy and Stage 2 computational overhead (e.g., latency and token consumption). This saturation suggests that top-5 candidates effectively prune most distractors, while remaining failures stem from inherent visual ambiguities rather than insufficient candidate quantity.

Effect of Different VLM and Prompting Strategies. As the reasoning core of Stage 2, the choice of VLM and the design of prompting strategies are critical for synthesizing multi-modal evidence. As summarized in Tab. 3, we first examine the contribution of each prompting component under a fixed VLM setting.

As shown in Table 3 (left), ablation experiments highlight the synergistic effect of spatial, semantic, and visual cues. Removing spatial relationship prompts leads to a performance drop from 54.0% / 40.3% to 51.6% / 38.1%, validating the

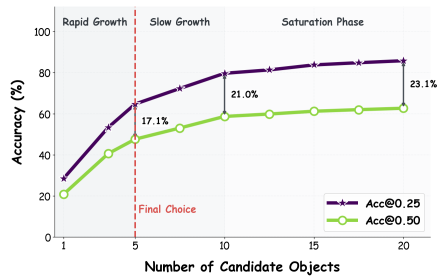


Fig. 7: Candidate count in Stage 1.

Table 3: Ablation studies of Stage 2 components. The left table evaluates the impact of prompting modules (Spatial, Semantic, and Visual CoT) using GPT-5. The right table compares the performance across various VLM backbones.

Spa.	Sem.	Vis.	Acc@0.25	Acc@0.5	VLM Backbone	Acc@0.25	Acc@0.5
✓	✓	-	54.0	40.3	GPT-4o	41.6	31.6
-	✓	✓	51.6	38.1	GLM-4.5	42.8	31.2
✓	-	✓	33.3	19.6	Qwen-2.5	43.8	33.2
✓	✓	✓	56.2	41.0	GPT-5 (Ours)	48.9	36.6

necessity of explicit geometric frames for spatial reasoning. More critically, excluding candidate-centric semantic evidence results in a sharp decline to 33.3% / 19.6%, proving that global visual renderings alone are insufficient for fine-grained discrimination. Optimal performance of 56.2% / 41.0% is achieved only when all components are integrated within our structured reasoning protocol, underscoring their collective importance for precise grounding.

As shown in Table 3 (right), beyond prompt engineering, grounding performance scales consistently with model capacity under identical configurations. GPT-5 achieves a state-of-the-art 48.9% / 36.6%, significantly outperforming Qwen-2.5 (43.8% / 33.2%) and GLM-4.5 (42.8% / 31.2%). This substantial margin—particularly the 5.1% absolute gain in Acc@0.25 indicates that fine-grained localization is inherently reasoning-intensive, requiring the superior representational depth of advanced foundation models to resolve spatial ambiguities. These results suggest that the primary bottleneck in visual grounding shifts from surface-level prompting to the intrinsic cognitive limits of the VLM backbone.

5 Conclusion

In this paper, we present UniGround, a training-free framework for open-world zero-shot 3D visual grounding that decouples geometric perception from semantic reasoning. By replacing domain-specific 3D detection with a training-free Global Candidate Filtering stage, UniGround constructs topology-aware scene representations without relying on any 3D supervision, unlocking true open-world generalization. The subsequent Local Precision Grounding stage introduces a structured reasoning protocol that synthesizes candidate-centric visual evidence with global spatial relationship prompts, enabling the VLM to perform precise, hallucination-free localization. Experimental results on ScanRefer and EmbodiedScan demonstrate that UniGround not only produces strong performance among zero-shot methods but also outperforms fully supervised baselines in complex, out-of-distribution scenarios. Furthermore, we provide the first demonstration of a zero-shot 3DVG system successfully deployed in real-world environments, validating its robustness against domain shifts. We hope our work inspires future research into training-free, reasoning-centric paradigms for more generalizable embodied perception.

References

1. Achlioptas, P., Abdelreheem, A., Xia, F., Elhoseiny, M., Guibas, L.: Referit3d: Neural listeners for fine-grained 3d object identification in real-world scenes. In: European conference on computer vision. pp. 422–440. Springer (2020)
2. Bolya, D., Huang, P.Y., Sun, P., Cho, J.H., Madotto, A., Wei, C., Ma, T., Zhi, J., Rajasegaran, J., Rasheed, H., et al.: Perception encoder: The best visual embeddings are not at the output of the network. arXiv preprint arXiv:2504.13181 (2025)
3. Chen, D.Z., Chang, A.X., Nießner, M.: Scanrefer: 3d object localization in rgb-d scans using natural language. In: European conference on computer vision. pp. 202–221. Springer (2020)
4. Dai, Z., Asgharivaskasi, A., Duong, T., Lin, S., Tzes, M.E., Pappas, G., Atanasov, N.: Optimal scene graph planning with large language model guidance. In: 2024 IEEE International Conference on Robotics and Automation (ICRA). pp. 14062–14069. IEEE (2024)
5. Guo, W., Xu, X., Wang, Z., Feng, J., Zhou, J., Lu, J.: Text-guided sparse voxel pruning for efficient 3d visual grounding. In: Proceedings of the Computer Vision and Pattern Recognition Conference. pp. 3666–3675 (2025)
6. Huang, R., Yang, H., Cai, Y., Xu, X., Zhang, H., He, S.: Viewsr: 3d visual grounding via structured multi-view decomposition. In: Proceedings of the IEEE/CVF International Conference on Computer Vision. pp. 9726–9736 (2025)
7. Huang, T., Zhang, Z., Tang, H.: 3d-r1: Enhancing reasoning in 3d vlms for unified scene understanding. arXiv preprint arXiv:2507.23478 (2025)
8. Huang, W., Wang, Z., Wei, Z., Huang, T., Zhao, F., Yang, J., Zhang, Z.: Open-ground: Active cognition-based reasoning for open-world 3d visual grounding. arXiv preprint arXiv:2512.23020 (2025)
9. Jain, A., Gkanatsios, N., Mediratta, I., Fragkiadaki, K.: Bottom up top down detection transformers for language grounding in images and point clouds. In: European Conference on Computer Vision. pp. 417–433. Springer (2022)
10. Jin, Z., Tu, R.C., Liao, J., Sun, W., Luo, X., Liu, S., Tao, D.: Spazer: Spatial-semantic progressive reasoning agent for zero-shot 3d visual grounding. arXiv preprint arXiv:2506.21924 (2025)
11. Kerr, J., Kim, C.M., Goldberg, K., Kanazawa, A., Tancik, M.: Lrf: Language embedded radiance fields. In: Proceedings of the IEEE/CVF international conference on computer vision. pp. 19729–19739 (2023)
12. Kirillov, A., Mintun, E., Ravi, N., Mao, H., Rolland, C., Gustafson, L., Xiao, T., Whitehead, S., Berg, A.C., Lo, W.Y., et al.: Segment anything. In: Proceedings of the IEEE/CVF international conference on computer vision. pp. 4015–4026 (2023)
13. Kong, L., Liu, Y., Chen, R., Ma, Y., Zhu, X., Li, Y., Hou, Y., Qiao, Y., Liu, Z.: Rethinking range view representation for lidar segmentation. In: Proceedings of the IEEE/CVF International Conference on Computer Vision. pp. 228–240 (2023)
14. Kong, L., Liu, Y., Li, X., Chen, R., Zhang, W., Ren, J., Pan, L., Chen, K., Liu, Z.: Robo3d: Towards robust and reliable 3d perception against corruptions. In: Proceedings of the IEEE/CVF International Conference on Computer Vision. pp. 19994–20006 (2023)
15. Li, J., Wang, H., Chen, J., Liu, Y., Dou, Z., Ma, Y., Yang, S., Li, Y., Wang, W., Dong, Z., et al.: Cityanchor: City-scale 3d visual grounding with multi-modality llms. In: ICLR (2025)

16. Li, R., Cao, A.Q., de Charette, R.: Coarse3d: Class-prototypes for contrastive learning in weakly-supervised 3d point cloud segmentation. arXiv preprint arXiv:2210.01784 (2022)
17. Li, R., Li, S., Kong, L., Yang, X., Liang, J.: Seeground: See and ground for zero-shot open-vocabulary 3d visual grounding. In: Proceedings of the Computer Vision and Pattern Recognition Conference. pp. 3707–3717 (2025)
18. Lin, J., Bian, S., Zhu, Y., Tan, W., Zhang, Y., Xie, Y., Qu, Y.: Seqvlm: Proposal-guided multi-view sequences reasoning via vlm for zero-shot 3d visual grounding. In: Proceedings of the 33rd ACM International Conference on Multimedia. pp. 3094–3103 (2025)
19. Lin, Z., He, S., Tan, C., Wen, B.: Groundflow: A plug-in module for temporal reasoning on 3d point cloud sequential grounding. In: Proceedings of the IEEE/CVF International Conference on Computer Vision. pp. 28774–28784 (2025)
20. Liu, Y., Mei, H., Zhan, D., Zhao, J., Zhou, D., Dong, B., Yang, X.: View-on-graph: Zero-shot 3d visual grounding via vision-language reasoning on scene graphs. arXiv preprint arXiv:2512.09215 (2025)
21. Liu, Z., Jia, W., Yang, M., Luo, P., Guo, Y., Tan, M.: Deep view synthesis via self-consistent generative network. *IEEE Transactions on Multimedia* **24**, 451–465 (2021)
22. Liu, Z., Yang, B., Luximon, Y., Kumar, A., Li, J.: Raydf: neural ray-surface distance fields with multi-view consistency. arXiv preprint arXiv:2310.19629 (2023)
23. Liu, Z., Ye, W., Luximon, Y., Wan, P., Zhang, D.: Unleashing the potential of multi-modal foundation models and video diffusion for 4d dynamic physical scene simulation. In: Proceedings of the Computer Vision and Pattern Recognition Conference. pp. 11016–11025 (2025)
24. Papon, J., Abramov, A., Schoeler, M., Worgotter, F.: Voxel cloud connectivity segmentation-supervoxels for point clouds. In: Proceedings of the IEEE conference on computer vision and pattern recognition. pp. 2027–2034 (2013)
25. Peng, S., Genova, K., Jiang, C., Tagliasacchi, A., Pollefeys, M., Funkhouser, T., et al.: Openscene: 3d scene understanding with open vocabularies. In: Proceedings of the IEEE/CVF conference on computer vision and pattern recognition. pp. 815–824 (2023)
26. Qi, Z., Zhang, Z., Fang, Y., Wang, J., Zhao, H.: Gpt4scene: Understand 3d scenes from videos with vision-language models. arXiv preprint arXiv:2501.01428 (2025)
27. Qian, Z., Ma, Y., Lin, Z., Ji, J., Zheng, X., Sun, X., Ji, R.: Multi-branch collaborative learning network for 3d visual grounding. In: European Conference on Computer Vision. pp. 381–398. Springer (2024)
28. Takmaz, A., Fedele, E., Sumner, R.W., Pollefeys, M., Tombari, F., Engelmann, F.: Openmask3d: Open-vocabulary 3d instance segmentation. arXiv preprint arXiv:2306.13631 (2023)
29. Unal, O., Sakaridis, C., Saha, S., Van Gool, L.: Four ways to improve verbo-visual fusion for dense 3d visual grounding. In: European Conference on Computer Vision. pp. 196–213. Springer (2024)
30. Wang, T., Mao, X., Zhu, C., Xu, R., Lyu, R., Li, P., Chen, X., Zhang, W., Chen, K., Xue, T., et al.: Embodiedscan: A holistic multi-modal 3d perception suite towards embodied ai. In: Proceedings of the IEEE/CVF Conference on Computer Vision and Pattern Recognition. pp. 19757–19767 (2024)
31. Wang, Y., Li, Y., Wang, S.: G³-LQ: Marrying hyperbolic alignment with explicit semantic-geometric modeling for 3d visual grounding. In: Proceedings of the IEEE/CVF Conference on Computer Vision and Pattern Recognition. pp. 13917–13926 (2024)

32. Wang, Y., Fang, Y., Wang, T., Feng, Y., Tan, Y., Zhang, S., Liu, P., Ji, Y., Xu, R.: Dreamnav: A trajectory-based imaginative framework for zero-shot vision-and-language navigation. arXiv preprint arXiv:2509.11197 (2025)
33. Wang, Y., Feng, Y., Fang, Y., Zhang, S., Jing, T., Li, J., Jiang, X., Xu, R.: Hero: Hierarchical traversable 3d scene graphs for embodied navigation among movable obstacles. arXiv preprint arXiv:2512.15047 (2025)
34. Wu, Y., Cheng, X., Zhang, R., Cheng, Z., Zhang, J.: Eda: Explicit text-decoupling and dense alignment for 3d visual grounding. In: Proceedings of the IEEE/CVF conference on computer vision and pattern recognition. pp. 19231–19242 (2023)
35. Xu, R., Huang, Z., Wang, T., Chen, Y., Pang, J., Lin, D.: Vlm-grounder: A vlm agent for zero-shot 3d visual grounding. In: Conference on Robot Learning. pp. 3961–3985. PMLR (2025)
36. Yin, Y., Liu, Y., Xiao, Y., Cohen-Or, D., Huang, J., Chen, B.: Sai3d: Segment any instance in 3d scenes. In: Proceedings of the IEEE/CVF Conference on Computer Vision and Pattern Recognition. pp. 3292–3302 (2024)
37. Yuan, Z., Ren, J., Feng, C.M., Zhao, H., Cui, S., Li, Z.: Visual programming for zero-shot open-vocabulary 3d visual grounding. In: Proceedings of the IEEE/CVF Conference on Computer Vision and Pattern Recognition. pp. 20623–20633 (2024)
38. Yuan, Z., Yan, X., Liao, Y., Zhang, R., Wang, S., Li, Z., Cui, S.: Instancerefer: Cooperative holistic understanding for visual grounding on point clouds through instance multi-level contextual referring. In: Proceedings of the IEEE/CVF International Conference on Computer Vision. pp. 1791–1800 (2021)
39. Zhang, J., Wang, K., Xu, R., Zhou, G., Hong, Y., Fang, X., Wu, Q., Zhang, Z., Wang, H.: Navid: Video-based vlm plans the next step for vision-and-language navigation. arXiv preprint arXiv:2402.15852 (2024)
40. Zhang, Y., Gong, Z., Chang, A.X.: Multi3drefer: Grounding text description to multiple 3d objects. In: Proceedings of the IEEE/CVF International Conference on Computer Vision. pp. 15225–15236 (2023)
41. Zhang, Z., Dai, W., Wen, H., Yang, B.: Logosp: Local-global grouping of super-points for unsupervised semantic segmentation of 3d point clouds. In: Proceedings of the IEEE/CVF Conference on Computer Vision and Pattern Recognition. pp. 1374–1384 (2025)
42. Zhang, Z., Yang, B., Wang, B., Li, B.: Growsp: Unsupervised semantic segmentation of 3d point clouds. In: Proceedings of the IEEE/CVF Conference on computer vision and pattern recognition. pp. 17619–17629 (2023)
43. Zhao, L., Cai, D., Sheng, L., Xu, D.: 3dvg-transformer: Relation modeling for visual grounding on point clouds. In: Proceedings of the IEEE/CVF International Conference on Computer Vision. pp. 2928–2937 (2021)
44. Zhou, G., Hong, Y., Wu, Q.: Navgpt: Explicit reasoning in vision-and-language navigation with large language models. In: Proceedings of the AAAI Conference on Artificial Intelligence. vol. 38, pp. 7641–7649 (2024)
45. Zhu, C., Zhang, W., Wang, T., Liu, X., Chen, K.: Object2scene: Putting objects in context for open-vocabulary 3d detection. arXiv preprint arXiv:2309.09456 (2023)
46. Zhu, Z., Ma, X., Chen, Y., Deng, Z., Huang, S., Li, Q.: 3d-vista: Pre-trained transformer for 3d vision and text alignment. In: Proceedings of the IEEE/CVF International Conference on Computer Vision. pp. 2911–2921 (2023)